

Polysulfide Networks. In Situ Formation and Characterization of the Elastomeric Behavior

Giona Kilcher,[†] Lei Wang,[†] Craig Duckham,[‡] and Nicola Tirelli^{*,†}

School of Pharmacy and Pharmaceutical Sciences, University of Manchester, Oxford Road, Manchester, M13 9PT, U.K., and Micap plc, Pemberton, Wigan, WN5 8AA, U.K.

Received January 23, 2007; Revised Manuscript Received April 13, 2007

ABSTRACT: Polysulfides with narrow polydispersity and variable chain length and density of polymerizable units have been synthesized through the use of a methacrylate-bearing and thiol-reactive compound as an end-capper for episulfide anionic polymerization. These macromonomers have been photopolymerized to yield materials with controlled cross-linking density, which translates into a controlled number of cross-links, branching points, and dead-ends. The resulting networks show elastomeric behavior that can be easily described through a simple affine chain model; in the analysis of the network behavior we here also present the calculation of a solvent-independent parameter for rationalizing the behavior of the Flory–Huggins parameters. These materials combine simple preparation (\rightarrow in situ processes), easy description of the mechanical properties, and responsiveness (to oxidation—not studied here), features that could make them attractive for biomedical applications.

Introduction

In an effort aiming to develop inflammation-responsive materials, we have focused our attention on polymer structures that can undergo chemical and, as a result, also morphological transitions in an oxidative environment, which is typical of many inflammatory reactions. The responsiveness of these systems is based on the conversion of hydrophobic organic sulfides (more specifically poly(1,2-alkylene sulfide)s, hereafter referred to as polysulfides) into hydrophilic sulfoxides or sulfones, generating a dramatic change in polarity in the material that can be conveniently used for triggering the release of loaded drugs.

In the past, we have mostly tackled the development of polysulfide-based nanostructures with the aim to produce circulating, inflammation-sensitive carriers, such as polymer vesicles¹ and nanoparticles.² The same approach could be applied to macroscopic (and hydrophobic) matrices that may be employed, e.g., as wound dressings or as (recoverable) implants for the topical and responsive treatment of inflammatory processes.

In this case, however, there are two issues to solve: (a) at physiologically acceptable temperatures most aliphatic polysulfides are well above their T_g (for a low MW poly(propylene sulfide) T_g can be as low as $-60\text{ }^\circ\text{C}$, while $T_{g\infty} \approx -35\text{ }^\circ\text{C}$), in a word they are viscous oils instead of solid matrices. b) ideally, macroscopic matrices should be amenable to preparation through mild and rapid hardening processes, which would allow their preparation at the site of application, e.g., for producing a conformal coating, for filling a cavity.

Polysulfides could therefore be seen as injectable liquid precursors, which are to be in situ transformed into a 3D elastic matrix. In order to minimize the precursors viscosity (and therefore improve their injectability), their molecular weight should be controlled and low; on the other hand, the hardening process must be based on the formation of covalent cross-links, since a physical gel of low MW polymers would lack of stability

(temperature and dilution may easily dissolve the components). A number of processes for producing covalent networks have been applied with good results in biological environment; as common features, they must show rapid kinetics, negligible temperature increase, no byproduct, no toxic intermediate, and negligible interference with biomolecules.

Photopolymerization reactions satisfy most of these criteria and indeed have been found to have application in this field,^{4,5} however mostly to produce hydrophilic materials. On the other hand, it is when dealing with hydrophobes that photopolymerization may have a distinct advantage over other (thermal) processes: most step-growth-based cross-linking reactions used for the in situ production of biomaterials are indeed based on polar intermediates (e.g., in Michael-type addition and disulfide formation the active species are deprotonated thiols), whose limited solubility in a hydrophobic phase sets limits to the cross-linking kinetics and can cause heterogeneities in the material.

We have therefore produced methacrylate-terminated polysulfide macromonomers and characterized the properties of the cross-linked elastomers obtained through their photoinitiated radical polymerization. Specifically, we have synthesized macromonomers with constant MW but a variable density of polymerizable groups for a fine control over the cross-linking density.

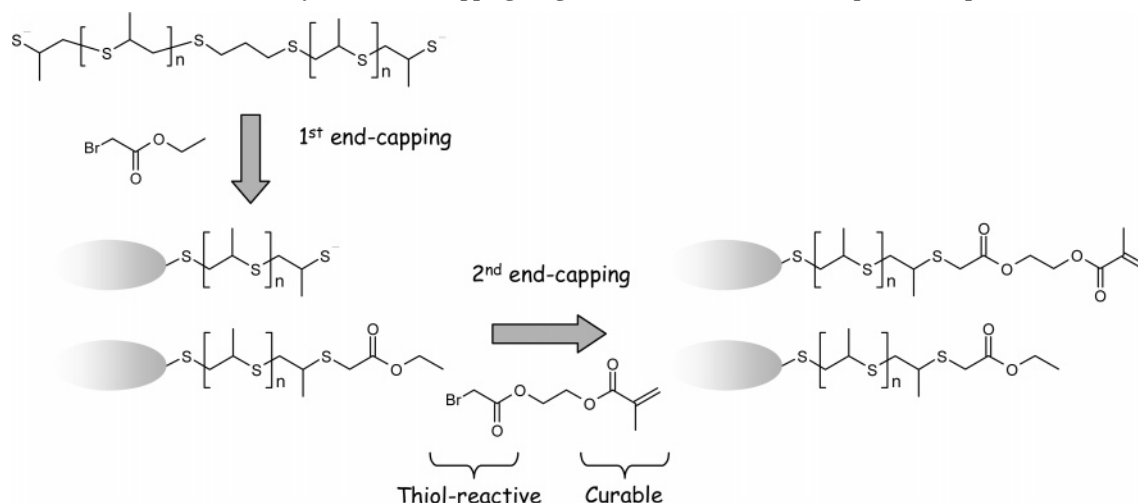
This was achieved by developing an ad hoc end-capping agent (BAEMA) that could be used at the end of episulfide polymerization for introducing methacrylates at the termini of polysulfide chains. (a) It is noteworthy that thiolates react with acrylates or methacrylates (Michael-type addition). We have therefore designed an end-capping agent that flanks a methacrylate (due to sterical hindrance methacrylates react with thiols slower than acrylates) with a much faster thiol-reactive group (2-bromoacetate). (b) In order to further decrease the likelihood of thiolate addition onto double bonds, this end-capper should be used in stoichiometric excess: a 1:1 ratio would mean that when most thiolates have reacted there would be a large excess of methacrylates compared to 2-bromoesters. Therefore, another, nonfunctional end-capper was added prior to BAEMA, in order precisely define the number of thiolates available for the functional end-capping.

The end-capping sequence is shown in Scheme 1.

* To whom correspondence should be addressed. E-mail: nicola.tirelli@manchester.ac.uk.

[†] School of Pharmacy and Pharmaceutical Sciences, University of Manchester.

[‡] Micap plc.

Scheme 1. Polysulfide End-Capping Stage, Which Consists of Two Sequential Steps^a

^a First is the addition of a stoichiometric defect of ethyl 2-bromoacetate, which is followed by that of 2-(bromoacetoxymethyl)ethyl methacrylate (BAEMA). This functional end-capping agent is added in 1.5 times molar excess in order to minimize the possibility of thiolate addition to double bonds.

Experimental Section

Materials. All materials were used as received from the supplier (Aldrich, Gillingham, U.K., for 2-hydroxyethyl methacrylate, propylene sulfide, 1,8-Diazabicyclo undec-7-ene, triethylamine, (±)-camphorquinone; Fluka, Gillingham, U.K., for ethyl bromoacetate and bromoacetyl bromide). THF was degassed by bubbling argon under inert atmosphere for 1 h before use.

Abbreviations: propylene sulfide, PS; triethylamine, TEA; 1,8-diazabicyclo[5.4.0]undec-7-ene, DBU; ethyl bromoacetate, EBA; (±)-camphorquinone, CQ; 2-(2-bromoacetoxymethyl)ethyl methacrylate, BAEMA.

Molecular Characterization. ¹H NMR spectra were recorded on a 300 MHz Bruker spectrometer. FT-IR spectra were recorded in ATR mode (Golden gate) on a Tensor 27 Bruker spectrometer. GPC was performed in THF on a Polymer Laboratories GPC 50 equipped with refractive index and viscosity detectors, using universal calibration with poly(styrene) standards.

End-Capper and Polymer Synthesis. Methacrylate Bearing End-Capper (BAEMA, 2-(2-Bromoacetoxymethyl)ethyl methacrylate). 2-Hydroxyethyl methacrylate (10.5 g, 82.5 mmol) was dissolved in 500 mL of THF under inert argon atmosphere. The solution was then cooled to 0 °C, and 1.8 equiv of triethylamine (15.0 g, 148.5 mmol) was added under stirring. In a dropping funnel 1.2 equiv of bromoacetyl bromide (20.0 g, 99.0 mmol) was first diluted with 50 mL of THF and then added dropwise to the reaction mixture. The mixture was allowed to react for 3 h, slowly being brought to room temperature. After filtration and evaporation of the solvent, the crude product was dissolved in CH₂Cl₂ (300 mL) and extracted three times with water and corrected to neutral pH by addition of NaHCO₃. The organic phase was then dried over Na₂SO₄ and subsequently treated with activated charcoal for 20 min. After evaporation of the solvent, the brown product was purified by flash chromatography with CH₂Cl₂ over neutral alumina (Al₂O₃), yielding a colorless liquid (6.54 g, yield 32%).

¹H NMR (CDCl₃): δ = 1.88 (s, 3H, CH₃ methacrylate), 3.70 (s, 2H, BrCH₂COO-), 4.25–4.40 (broad multiplet, 4H, COO-CH₂-CH₂-OCO-), 5.53 (s, 1H, cis H methacrylate), 6.07 (s, 1H, trans H methacrylate).

ATR-IR (thin film): 2958 (ν_{as}(CH₃)), 2919 (ν_{as}(CH₂)), 2867 (ν_s(CH₃)), 1737 (ν(C=O) saturated aliphatic ester), 1717(ν(C=O) α,β-unsaturated aliphatic ester), 1637 (ν(C=C)), 1450 and 1372 (δ_{as} and δ_s CH₃ bending), 1163 cm⁻¹ (ν(CC(=O)-O)).

Homo- and Hetero-Capped Linear Poly(propylene sulfide). The polymers used in this study were prepared in parallel experiments in a Omni 6 parallel reactor (Thermo Electron) at room temperature under argon atmosphere.

Typically, series of polymerization experiments were run in parallel to yield families of polymers with identical molecular weight (constant monomer/initiator ratio) but different ratios between polymerizable and nonpolymerizable end-capping groups. 1,3-dimercaptopropane (DMP) and propylene sulfide (PS) were dissolved under inert atmosphere in degassed THF to prepare a stock solution with a fixed ratio between monomer and initiator (e.g., containing 20 mg/mL of DMP and 275 mg/mL of PS for a 1:20 molar ratio, corresponding to a 1:10 thiol-to-monomer ratio). Then, 20 mL of stock solution was introduced under inert argon atmosphere in a reactor. The polymerization was then started by adding the required amount of 300 mg/mL THF solution of DBU for a 1:1 DBU/thiol ratio. The reagents were allowed to react for 45 min, and then to each reactor was added a different quantity of ethyl bromoacetate (EBA) (for an EBA/thiol ratio of 0.75/1, 0.5/1, 0.35/1, 0.2/1 and 0/1). After additional 2 h, a THF stock solution (200 mg/mL) of 2-(bromoacetoxymethyl)ethyl methacrylate (BAEMA) was added to each reactor in variable quantity to provide a 1.5 times molar excess of BAEMA to the remaining thiolates (BAEMA/thiol ratio of 0.37/1, 0.75/1, 0.97/1, 1.2/1 and 1.5/1). The mixture was allowed to react for a further 2 h and then filtered over glass wool and evaporated at the rotary evaporator. The crude product was then redissolved in 30 mL CH₂Cl₂, extracted three times with 6 mL of water, and then dried over Na₂SO₄. The solvent was completely removed at the rotatory evaporator and the oily polymer was extracted 3 times with 5 mL MeOH. After sedimentation from the MeOH solution, the polymer was separated and dried for 24 h under reduced pressure. A viscous colorless oil (average yield 65–70%) was finally collected.

¹H NMR (CDCl₃): δ = 1.26–1.30 (t, CH₃CH₂COO-), 1.35–1.37 (d, CH₃ in PPS chain), 1.80–1.90 (q, 2H, in S-CH₂-CH₂-CH₂-S-), 1.94 (s, 3H, CH₃ methacrylate), 2.51–2.61 (m, 1 diastereotopic H of CH₂ in PPS chain), 2.75–2.93 (m, CH and 1 diastereotopic H of CH₂ in PPS chain), 3.20–3.37 (m, 4H, -S-CH₂-COO-), 4.15–4.20 (q, 2H, CH₃CH₂COO-), 4.37 (broad s, 4H, CH₂=CH(CH₃)COO-CH₂-CH₂-COO-), 5.6 (s, 1H, cis H methacrylate), 6.1 (s, 1H, trans H methacrylate) ppm.

ATR-IR (thin film): 2958 (ν_{as}(CH₃)), 2919 (ν_{as}(CH₂)), 2867 (ν_s(CH₃)), 1737 (ν(C=O) saturated aliphatic ester), 1717(ν(C=O) α,β-unsaturated aliphatic ester), 1637 (ν(C=C)), 1450 and 1372 (δ_{as} and δ_s CH₃ bending), 1163 (ν(CC(=O)-O)), 1173 (ν(C-S) in PPS) cm⁻¹.

Photopolymerization Experiments. Preparation of Macroscopic Samples for Swelling Experiments. Samples of hetero end-capped poly(propylene sulfide)-α-methacrylate-ω-ethylacetate were introduced in a 1.5 mL centrifuge tube and an amount of stock solution of (±)-camphorquinone (CQ) in dichloromethane (500 mg/

mL) was deposited on the surface of the viscous material in order to obtain a final concentration of 1 wt % CQ and evaporated at reduced pressure in a vacuum oven for 10 min. At this point the sample displayed a viscous, colored layer of initiator with a limited mixing with the underlying, oily polymer; the penetration was then facilitated by centrifugation of the tubes for 10 min at 10K rpm (the layer disappears and the sample becomes homogeneously colored) and then mixing, first manually and then with an orbital shaker at 200 rpm for 10 min, to ensure complete homogenization. The mixtures were stored at 4 °C and protected from light before use. Cylindrically shaped samples were prepared by pouring the viscous mixture into a Teflon mold of 4 mm diameter, which was closed with transparent polycarbonate films; they were then cured by irradiation for 200 s from each side with a blue led light (peak maximum at 460 nm, L.E.Demetron I, kindly donated by Ker-Hawe, Switzerland) at 800 mW/cm².

The cross-linked polysulfide cylinders (4 mm diameter, 2 mm thickness) were immersed in 1 mL dichloromethane and allowed to equilibrate for 2 h at 25 °C. The swollen objects were then removed from the vial and gently mopped with a tissue paper prior to determine their wet weight. The objects were then dried over reduced pressure overnight, and then their dry weight was determined; the weight swelling index was calculated from the ratio between the wet weight and the dry weight of the gel.

Photopolymerization Experiments Followed by Shear Rheometry. Polymer films were studied and cured in a UV-cell of a Bohlin Gemini shear rheometer in parallel plate geometry. The light was conveyed into the UV-cell by an optical fiber guide irradiating the sample through the quartz bottom plate, on the top of which the viscous macromonomers and photoinitiator mixture was placed. The oscillating plate (25 mm diameter) was placed at a fixed gap of 100 μ m from the bottom quartz plate. The output of the guide was placed coaxially with the plate shaft to completely and homogeneously irradiate (with a 20 mW/cm² 460 nm light) the area covered by the oscillating plate.

The material was irradiated for 10 min while measuring G' and G'' (frequency 1 Hz and controlled stress amplitude of 10 Pa). After this was complete, a stress amplitude sweep at 1 Hz from 10 to 30 000 Pa was measured, in order to obtain the moduli in the linear (Newtonian) region.

Photopolymerization Experiments Followed by (ATR) FT-IR Spectroscopy. The viscous macromonomers and photoinitiator mixture was placed over a germanium (ATR) crystal and cured with blue led light ((with a 20 mW/cm² 460 nm light), interrupting irradiation every 20 s to acquire the IR spectra.

Results and Discussion

Preparation of Homo- and Hetero-Capped Linear Poly(propylene sulfide). Choice and Preparation of a Functional End-Capper. We have previously employed the living, ring-opening anionic polymerization of episulfides for the preparation of linear⁶ or cross-linked homo-⁷ and block copolysulfides.⁸ Both the initiators⁹ and the propagating species are deprotonated thiol-based nucleophiles (thiolates); their fairly low basicity (low pK_a of the protonated counterpart), unlike the propagating species of most other anionic polymerizations, makes the presence of water not a problem in itself, since protonation and chain termination can be avoided by the use of an appropriate pH (e.g., pH > pK_a + 2); therefore, extremely anhydrous conditions are not required (the polymerization can be conducted in water emulsion too). However, not only thiolates are insensitive to the presence of water; they also tolerate a number of other groups (e.g., alcohols, amines, esters, amides) possibly present in bioactive or chemically reactive structures, while they can undergo a range of selective reactions, e.g., toward electron-poor unsaturated groups (Michael-type addition onto acrylates and related compounds¹⁰) or halides (nucleophilic substitution onto bromides and iodides, in particular when close to electron-

Table 1. Characterization Data for Homo- and Hetero-End-Capped Polysulfides

sample	feed		¹ H NMR		GPC ^c			η^* (Pa·s)
	PS/ I ^a	EBA/ RSH ^b	methacrylate molar fraction (λ) ^c	DP ^d	\overline{M}_n	\overline{M}_w	$\overline{M}_w/\overline{M}_n$	
P-11	10	1.00	0.00	13.0	1040	1280	1.23	0.81
P-12	10	0.85	0.14	13.3	1050	1250	1.19	0.90
P-13	10	0.60	0.40	14.5	1200	1440	1.20	0.98
P-14	10	0.45	0.52	13.8	1300	1580	1.22	1.08
P-15	10	0.30	0.71	14.6	1350	1600	1.19	1.06
P-16	10	0.10	0.91	13.0	1420	1700	1.20	1.59
P-21	20	1.00	0.00	19.5	1600	1920	1.20	2.42
P-22	20	0.75	0.32	19.8	1460	1720	1.18	2.92
P-23	20	0.60	0.42	21.1	1500	1780	1.19	1.77
P-24	20	0.35	0.68	19.5	1660	1980	1.19	3.05
P-25	20	0.20	0.77	20.8	1920	2320	1.21	4.11
P-26	20	0.00	1.00	19.8	1900	2300	1.21	3.38
P-41	40	1.00	0.00	39.7	3060	3700	1.21	3.97
P-42	40	0.75	0.24	38.5	2740	3100	1.13	3.95
P-43	40	0.50	0.46	37.6	2940	3440	1.17	5.15
P-44	40	0.35	0.61	34.2	2940	3440	1.17	3.79
P-45	40	0.20	0.76	36.9	3040	3500	1.15	4.36
P-46	40	0.00	1.00	43.5	3100	3540	1.14	5.44

^a Ratio between the moles of propylene sulfide and 1,3-dimercaptopropane introduced into the feed (note that each 1,3-dimercaptopropane molecule bears two initiating species). ^b Ratio between the moles of the first end-capping agent introduced (ethyl bromoacetate) and the moles of thiols initially present in the feed. ^c Calculated as the ratio between the integral of a methacrylate proton (5.6 and 6.1 ppm) and the sum of that of methacrylate plus that of an ethyl acetate methylene proton (4.15–4.20 ppm). ^d Degree of polymerization of the chain, calculated as the ratio between the value of a PPS methyl proton (1.30 ppm) integral and (a) the half of an ethyl acetate methylene proton (4.15–4.20 ppm) for P-11, P-21 and P-41, or (b) half of the sum of the integrals of a proton in the two terminal groups (methacrylate and ethyl acetate) for the remaining polymers. ^e Calculated by the means of the universal calibration with polystyrene.

withdrawing groups). This therefore makes it possible to decorate the polysulfide chains with a number of functional groups through the use of appropriate end-cappers.

It is noteworthy that, while both Michael-type addition and nucleophilic substitution have been widely used for thiol functionalization,⁸ the second reaction can be much quicker than the first one; this is particularly true if Michael-type acceptor is even mildly sterically hindered, e.g., a methacrylate vs an acrylate.¹¹

For example, a molecule displaying both a methacrylate (sterical hindrance by the methyl group) and a 2-haloester can selectively react at the halide; it could thus be employed as an end-capper, at the same time introducing a polymerizable group at the polymer terminus. We have therefore prepared a molecule of this kind, 2-methacryloxyethyl-2'-bromoethanoate (BAEMA), from the reaction of hydroxyethyl methacrylate (HEMA) with bromoacetyl bromide.

Polymer Synthesis. We have prepared a family of polymers differing in molecular weight and/or in content of methacrylate (polymerizable) groups, which we express in Table 1 as methacrylate/ethyl acetate molar fraction. The preparation is based on a *one pot* sequence: deprotonation of 1,3-dimercaptopropane (bifunctional initiator), initiation and propagation of propylene sulfide polymerization, and finally end-capping of the two termini of the macromolecule.

By using a 1:1.5 thiolate:2-bromoester ratio, the terminal thiols selectively react with BAEMA α -bromoester, as shown by ¹H NMR spectroscopy (Figure 1), and no Michael-type addition on the double bond could be observed: the resonance of the α -carbon protons quantitatively shift from 3.7 (BrCH₂-COO-) to 3.30 ppm (-S-CH₂-COO-) (complete substitution of bromine by sulfur), while the integral of the vinylidene

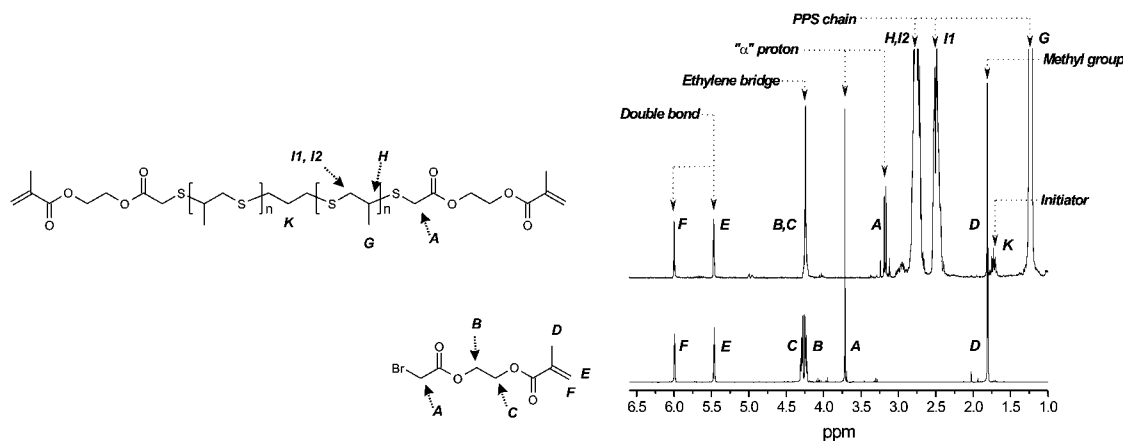


Figure 1. ¹H NMR spectra of BAEMA before and after the end-capping reaction. The reaction was conducted with a thiolate:bromoester 1:1.5 molar ratio.

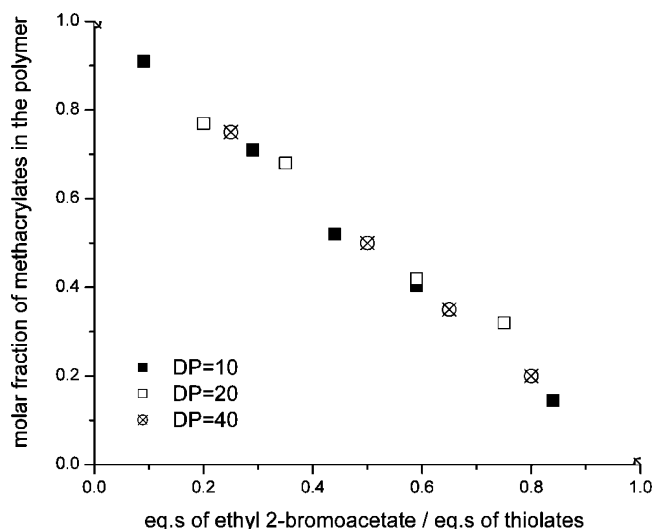


Figure 2. Molar fraction of methacrylate groups in the polymer (estimated from NMR) vs relative amount of the feed of the first end-capping agent. Their sum is constantly equal to one independently on the polymer MW, ensuring that (a) all ethyl 2-bromoacetate was incorporated, (b) all thiolates have reacted with one or the other reagent, and (c) the molecular weight (in the range investigated) does not have an important role in the reactivity of the terminal groups.

protons remains constant (when normalized to that of the ethylene protons **B** and **C**).

In a more general case, the density of polymerizable groups can be controlled through a two-step end-capping procedure (Scheme 1). First, we use a stoichiometric defect of ethyl 2-bromoacetate, leaving therefore a controlled amount of thiolates for further reactions and eventually determining the methacrylate/ethyl acetate molar fraction; the remaining thiolates are then reacted with BAEMA in 1.5 molar excess, the ratio previously shown to provide no reaction at the double bond. If ethyl 2-bromoacetate reacts in quantitative fashion and the remaining thiolates also quantitatively react with BAEMA, the molar fraction of methacrylate terminal groups would then correspond to 1 equiv of ethyl 2-bromoacetate per thiolate. This is in fact the case (Figure 2), and the methacrylate molar fractions always complement to one the ethyl 2-bromoacetate/thiol ratio used in the reaction. This linear relationship is independent of the polymer MW, showing all ethyl 2-bromoacetates to be incorporated and all thiolates to react.

Viscosity of Macromonomers (Injectability). All macromonomers have fairly high viscosity values, which depend mainly on the molecular weight and possibly, but much less

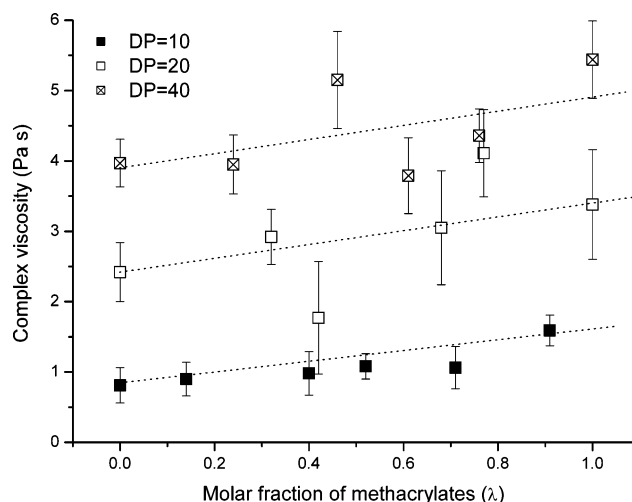


Figure 3. Viscosity of the macromonomers as a function of the degree of polymerization of the macromonomers and of the molar fraction of polymerizable groups. The dotted lines (obtained from a linear fit of the average values) are introduced only as a guide for the eyes and do not assume a linear dependence on the composition of the terminal groups.

sharply, on the composition of the terminal groups (Figure 3). These values are about 1 order of magnitude higher than those of a commonly used injectable solution for in situ hydrogel formation, such as 1 wt % sodium alginate in water.¹² This, however, does not really hinder the injectability of the macromonomers: other injectable solutions do show similar viscosity values (e.g., cellulose derivatives¹³), and furthermore, in our experience, we have not encountered any problem in applying these liquids even through the very narrow needles of 100 μ L Hamilton syringes.

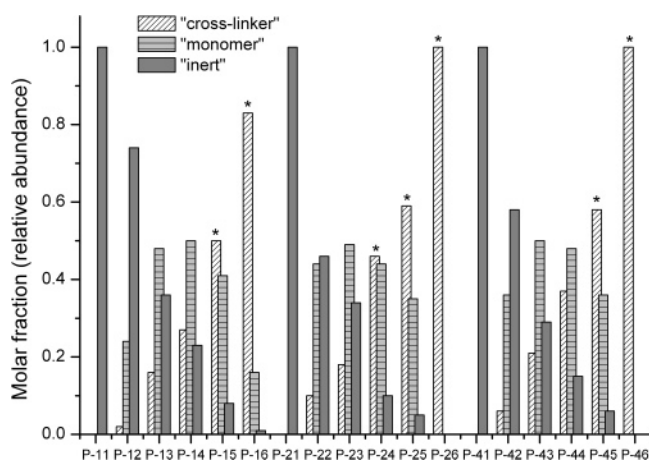
Polymer Mixtures. We will hereafter refer to the polymer chains containing two identical end groups as homo-capped chains, and to those with different end groups as hetero-capped chains.

We assume that during end-capping each terminal thiolate reacts independently (otherwise the data in Figure 2 should show some influence of the MW, i.e., of the distance between terminal groups); the molar fractions of methacrylate- and ethyl acetate-homo-capped and that of hetero-capped polymers can thus be estimated from the overall amount of methacrylates, λ (Table 2): they will, respectively, correspond to λ^2 , $(1 - \lambda)^2$, and $2\lambda(1 - \lambda)$.

It is noteworthy that methacrylate homo-capped chains will act as cross-linkers, while hetero-capped chains behave as

Table 2. Summary of the Composition of the Different Macromonomer Mixtures

polymer	theoretical (real) DP	λ	λ^2 ^a	$(1 - \lambda)^2$ ^b	$2\lambda(1 - \lambda)$ ^c
P-11	10 (13.0)	0.00	0.00	1.00	0.00
P-12	10 (13.3)	0.14	0.02	0.74	0.24
P-13	10 (14.5)	0.40	0.16	0.36	0.48
P-14	10 (13.8)	0.52	0.27	0.23	0.50
P-15	10 (14.6)	0.71	0.50	0.08	0.41
P-16	10 (13.0)	0.91	0.83	0.01	0.16
P-21	20 (19.5)	0.00	0.00	1.00	0.00
P-22	20 (19.8)	0.32	0.10	0.46	0.44
P-23	20 (21.1)	0.42	0.18	0.34	0.49
P-24	20 (19.5)	0.68	0.46	0.10	0.44
P-25	20 (20.8)	0.77	0.59	0.05	0.35
P-26	20 (19.8)	1.00	1.00	0.00	0.00
P-41	40 (39.7)	0.00	0.00	1.00	0.00
P-42	40 (38.5)	0.24	0.06	0.58	0.36
P-43	40 (37.6)	0.46	0.21	0.29	0.50
P-44	40 (34.2)	0.61	0.37	0.15	0.48
P-45	40 (36.9)	0.76	0.58	0.06	0.36
P-46	40 (43.5)	1.00	1.00	0.00	0.00

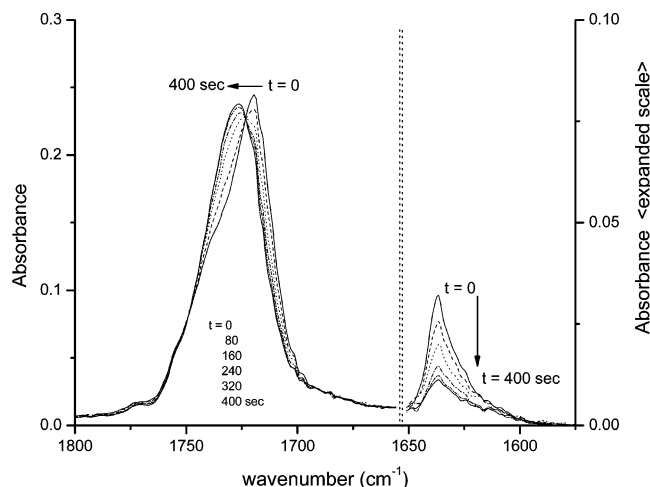
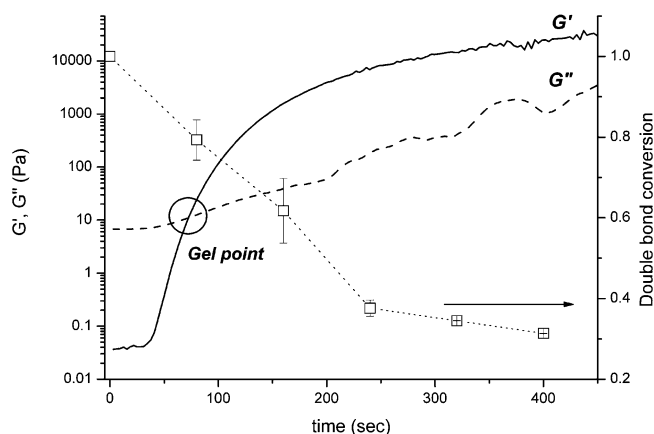
^a Molar fraction of methacrylate homo-capped polymers ("cross-linkers").^b Molar fraction of hetero-capped polymers ("monomers"). ^c Molar fraction of ethyl acetate homo-capped polymers ("plasticizers").**Figure 4.** Composition of the macromonomer mixtures used in this study (data from Table 2).

"monomers", while ethyl acetate homo-capped chains should not participate to the polymerization and would only be physically entrapped in the resulting networks.

Having in mind possible applications, ethyl acetate homo-capped chains should not be present, since they would be leachable components. In this study, however, we focus on the properties of photopolymerized cross-linked networks as a function of their cross-linking densities. The presence of a controlled number of non-cross-linked chains with identical composition (and therefore perfect miscibility) does not cause any problem to the analysis of, e.g., the mechanical properties; on the contrary, it is beneficial in that it allows a more precise control over the cross-linking density where this has low or very low values.

In future applications, only samples could be used that do not contain ethyl acetate homo-capped chains (and therefore present high cross-linking densities); they can be obtained from high λ samples (labeled with a star in Figure 4), by chromatographically removing the undesired homo-capped chains (silica as a stationary phase, eluted with 5:2 hexane:ethyl acetate).

Photopolymerization and Material Characterization. Conditions of Photopolymerization. The terminal methacrylates were polymerized through a photoinitiated free radical mechanism. After casting or molding the materials, we have employed

**Figure 5.** Changes in IR absorbance spectrum of P16 (91% of terminal groups are methacrylates) as a function of the irradiation time (light power 20 mW/cm²). The right part of the spectrum is reported with 3 times magnified scale to enhance the visibility of the disappearance of the C=C stretching vibration.**Figure 6.** Kinetics of photoinitiated cross-linking for P-16 followed by shear rheometry (frequency = 1 Hz) and IR (monitoring the double bond stretching decrease). The circle highlights the gel point, defined as where $G' \approx G''$ ($\approx \omega''$), i.e., where both moduli have the same frequency dependence and their ratio is frequency independent. It is noteworthy that the modulus at the gel point can be partially influenced by the initial value of G'' (and hence by the viscosity of the macromonomer mixture).

camphorquinone (CQ) as a photosensitized initiator (absorption maxima of CQ at 460 nm). IR spectra can be used for monitoring the polymerization kinetics by following the conversion of unsaturated groups (Figure 5) through the decrease of double bond stretching absorption (1636 cm⁻¹) and the shift of the ester stretching signal (1637–1618 cm⁻¹). Because of the rapid rate, however, only a few readings can be collected during polymerization, which allow to estimate final conversion and end point (respectively 70–75% and roughly 400 s, in agreement with shear rheometry data, Figure 6), but not, e.g., to ascertain whether a first-order kinetics is followed.

Generally, CQ is used in combination with amines, such as triethanolamine: the CQ excited-state produces a free radical by abstracting a hydrogen atom from the tertiary amine, thus generating the primary radical.¹⁴ In our case, however, we have not recorded any sound difference in polymerization rate and mechanical properties of the material in the presence (1 wt %) or absence of triethanolamine; this finding has induced us to believe that hydrogen radicals could be abstracted also from polysulfide chains. For seek of simplicity (reduction of com-

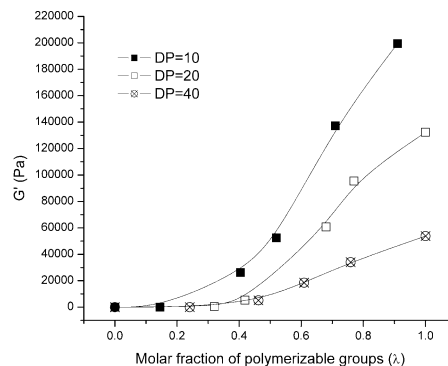
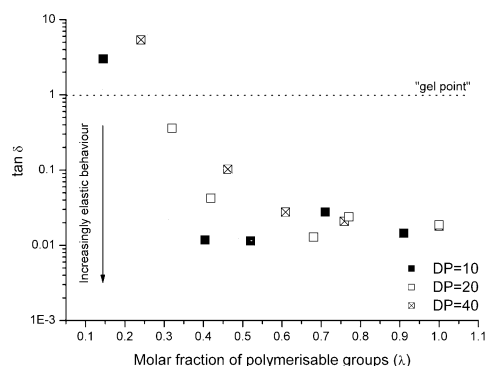


Figure 7. Left: Phase angle of the photopolymerized materials as a function of the density of polymerizable groups. The tendency to decrease indicates an increasingly elastic character. The dotted lines are just guides for an easier visual identification of the trend. Right: shear elastic modulus (G) as a function of the degree of polymerization of the macromonomers and of the molar fraction of polymerizable groups. Lines are only a guide for the eyes.

ponents is advantageous in view of a possible biomedical application), we have therefore made use of CQ only and initiated the free radical polymerization upon irradiation with a 20 mW/cm² blue light (maximum at 460 nm). Again, we have not recorded any sound effect of CQ concentration in the range 0.1 to 5 wt %; all the experiments here presented were thus performed at 1 wt %.

Rubber Elasticity of Polysulfide Networks. After irradiation, most samples show a predominantly elastic behavior ($\tan \delta < 1$, Figure 7, left), which is easy to visually correlate with λ , as shown in Figure 7, right.

G' data can be rationalized by using rubber elasticity theory: the shear modulus of a cross-linked material composed of flexible chains ($T > T_g$) is directly related to N_v , the number elementary chains building the network in a volume unit:

$$G = kTN_v \quad (\text{I})$$

It is important to point out that here we use an affine chain model, neglecting the influence of entanglements, which would require a model such as that of Langsley and Graessley:^{15,16} indeed the elastic modulus of the uncross-linked mixtures of macromonomers (the entanglement-related G_N^0 in the Langsley-Graessley approach) is indeed 3 to 5 orders of magnitude lower than those of our polymerized networks.

We also make the following assumptions:

(a) The chains with no or only one methacrylic group negligibly contribute to the overall value of the modulus; therefore, N_v corresponds to the number of cross-linkers reacted at both sides

(b) The shorter connections between cross-linking points are portions of methacrylic chains (the longer connections are the polysulfide chains), with a low number of possible conformations (hindered by the presence of the large polysulfide side chains). Since they exhibit a very limited entropic variation when deformed, we assume their influence on the rubber elasticity behavior to be negligible, therefore only polysulfide chains are taken into account and the molecular weight between cross-links \bar{M}_c can be expressed as the polysulfide chain $\bar{M}_n = \text{DP} \times \text{MW}_{\text{PS}}$ (degree of polymerization \times the molecular weight of the monomer).

Under these assumptions, the number of elementary chains can be derived from the total number of chains per units volume (equal to the density of the material \times the Avogadro's number, divided by the molecular weight between cross-links \bar{M}_c) multiplied by the relative molar fraction of the cross-linker in the polymer mixture (λ^2 , where λ is the molar fraction of

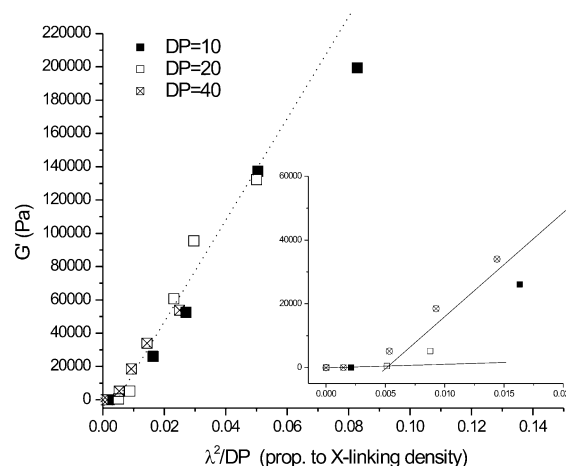


Figure 8. Shear elastic modulus (as in Figure 7, left), which depends linearly on the parameter λ^2/DP , which is directly proportional to the cross-linking density, since the conversion of polymerizable groups is almost identical for all samples after polymerization. The inset shows, however, that samples with $\lambda^2/\text{DP} < 0.005$ (which have $G'' > G'$) do not follow this behavior.

methacrylate) and by the probability that it has reacted at both sides (DC^2 , where DC is the degree of double bond conversion).

$$N_v = \lambda^2 (\text{DC})^2 N_a \rho / M_c \quad (\text{II})$$

Introducing these terms into eq I, the shear modulus then reads:

$$G = RT\rho\lambda^2(\text{DC})^2/(\text{DP} \times \text{MW}_{\text{PS}}) \quad (\text{III})$$

Since all our materials are characterized by a similar degree of conversion, the affine chain model would therefore predict a linear dependence of G on λ^2/DP . Indeed this is observed (Figure 8), indicating the substantially ideal (affine) elastomeric behavior of the polysulfide networks.

“Ideal” Behavior also during Polymerization. A closer look at Figure 8 (magnified part on the right) shows that a few samples, those with $\lambda^2/\text{DP} < 0.005$, do not cross the gel point.

In an idealized picture, the structure of a network during its formation should not be influenced by the different composition of terminal groups, nor by the kinetics of the curing reaction; macromonomers with identical DP and the same density of polymerized end groups (but possibly a different original content of methacrylates) should thus be present in the same kind of branched aggregates. In other words, the behavior of the network would be solely dictated by the number of cross-links and their distance.

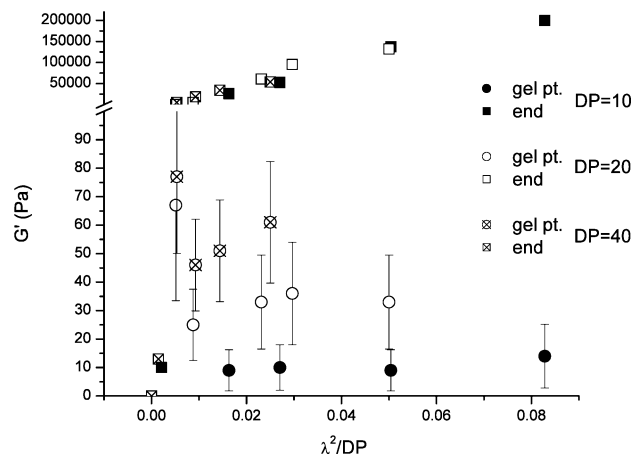


Figure 9. Shear elastic modulus at the gel point, which is substantially independent of λ^2/DP , while for most samples there seems to be a dependence on the length of the macromonomer. The final shear elastic moduli (same values as in Figure 8) are reported in the top part of the graph for comparison.

In this picture, all samples should feature the same, critical density of polymerized groups at the gel point. If the number of polymerized groups would be below this critical density, the sample would not be a gel.

This threshold could be calculated utilizing the samples at the intersection of the plot in Figure 8 (where $\lambda^2/\text{DP} = 0.005$), i.e., those where the gel point occurs very late in (“at the end of”) the photopolymerization process and thus the final double bond conversion is roughly the same as that at the gel point. For these samples, the critical value of the cross-link density can be approximated with its final one: $\lambda^2/\text{DP} \times \text{DC}^{\text{fin}} = 0.005 \times (0.7 \div 0.8) \approx 0.0035 \text{ mol/g}$, where DC^{fin} is the final conversion of methacrylates. Therefore, in an ideally behaving network, the conversion at the gel point could be calculated as $\text{DC}^{\text{gel}} \approx 0.0035\{\text{DP}/\lambda^2\}$.

This hypothesis could be validated if the two following conditions are true:

(a) If all the systems composed by macromonomers with the same chain length and the same density of polymerized groups (cross-links) are roughly identical throughout the curing and this density is constant at the gel point, then the modulus at the gel point ($G' = G'' = G^{\text{gel}}$) should be independent of λ^2/DP , but dependent on DP. This is indeed observed for most samples, although with large error bars (Figure 9). Please note that this is not a direct consequence of the elasticity theory, but simply follows from the fact that similar branched structures should show similar rheological behavior.

(b) If we suppose the photoinitiated polymerization to obey a pseudo first-order kinetics with a generic equation $\text{DC}(t) = A(1 - \exp(-(t - t_0)/\tau))$, the ideal behavior of the network as defined above would imply an exponential relationship between the parameter DP/λ^2 and the gel time:

$$\text{DC}^{\text{gel}} = A \left(1 - \exp \left(\frac{t^{\text{gel}} - t_0}{\tau} \right) \right) \rightarrow \frac{\text{DP}}{\lambda^2} = A' \left(1 - \exp \left(\frac{t^{\text{gel}} - t_0}{\tau} \right) \right)$$

The experimental data ($\{\text{DP}/\lambda^2\}$ vs t^{gel} in Figure 10) can indeed be fitted with this model, providing values of $A' = 227 \pm 12$, $\tau = 104 \pm 9 \text{ s}$, $t_0 = 51 \pm 5 \text{ s}$; the last two are in qualitative agreement with both IR and rheology data. The

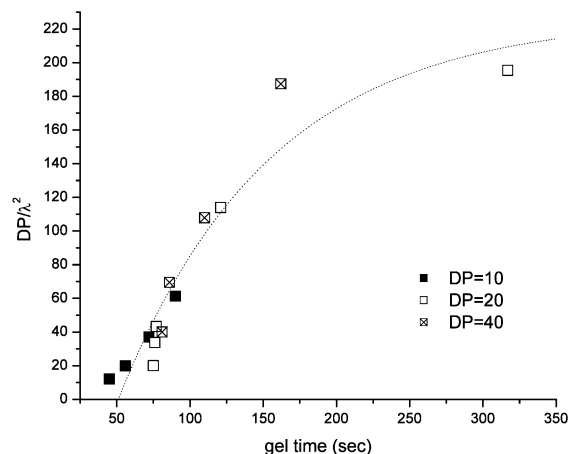


Figure 10. Relationship between DP/λ^2 and gel time. This is compatible with a polymerization mechanism with pseudo-first-order kinetics (such as that of radical polymerization).

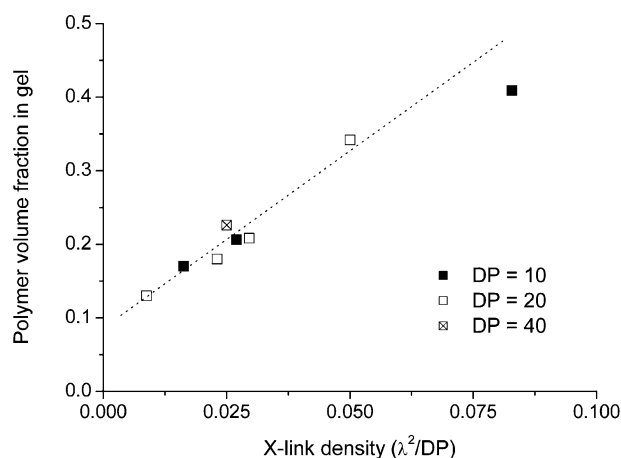


Figure 11. Polymer volume fraction as a function of λ^2/DP (where λ is the molar fraction of methacrylate and DP, the degree of polymerization of the macromonomer). At constant conversion, λ^2/DP is proportional to the number of elementary chains per unit volume.

presence of a time lag of about 50 s is easy to explain with the necessity to consume all oxygen dissolved in the samples before the radical polymerization can really start.

We do not want to stress the strict applicability of this fit, but simply that these qualitative data seem to support the hypothesis to have a roughly ideal behavior of the polymer chains during cross-linking, where their rheological properties can be substantially interpreted only on the basis of conversion of polymerizable groups and distance between them (i.e., cross-link density).

Swelling in Organic Solvent and Flory—Huggins Parameter. The discussion of these measurements should be anticipated by an important *caveat*. Our samples always contain a certain amount of nonreacted chains, which in the dry networks would act as a diluent, but could be solubilized in the presence of an excess solvent. We have therefore taken particular care in (a) using samples with less than 36% of unbound chains, (b) employing very small amounts of dichloromethane, and (c) redrying the samples after swelling in order to measure the weight loss, which has generally been negligible. The data used hereafter are indeed the weight differences between swollen and redried gels, since these values have higher reproducibility (lower error) than the weight difference with original gels, but no substantial difference.

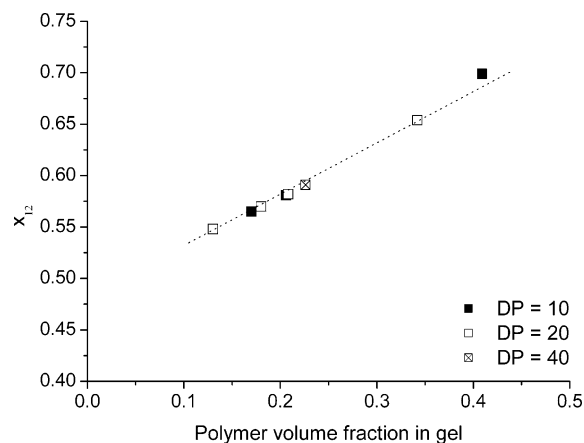


Figure 12. Flory–Huggins interaction parameter ($\chi_{1,2}$) as a function of the polymer volume fraction in equilibrium swollen gels (ϕ_{sw}).

In dichloromethane-swollen gels, the polymer volume fraction was derived from the weight polymer fraction (ratio between swollen and dry weight), assuming the gel density to be a linear combination between the density of the dry polymer and that of the solvent. Swelling decreases (the polymer volume fractions increases) linearly with increasing cross-link density of the dry networks, which in an affine scheme is linearly proportional to that of the swollen networks (Figure 11).

According to the so-called Frenkel–Flory–Rehner hypothesis, a network swells because of a negative ΔG associated with the mixing of the solvent with the polymer, and it is counteracted by the elastic behavior of the cross-links. We have applied the Flory–Rehner equation to relate the molecular weight between cross-links to the volume fraction of the polymer in the swollen gel.¹⁷

$$\frac{1}{M_C} = \frac{2}{M_n} - \frac{(\bar{v}/V_1)[\ln(1 - \phi_{sw}) + \phi_{sw} + \chi_{1,2}\phi_{sw}^2]}{\phi_{sw}^{1/3} - \phi_{sw}/2} \quad (\text{IV})$$

\bar{M}_n is the number-average molecular weight of the polysulfide chain and, as we have previously discussed, we assume $\bar{M}_n = M_C$; \bar{v} is the specific volume of the polymer, V_1 is the specific volume of the swelling agent, ϕ_{sw} is the polymer volume fraction in the equilibrium swollen gel, and $\chi_{1,2}$ is the Flory–Huggins interaction parameter between network and dichloromethane.

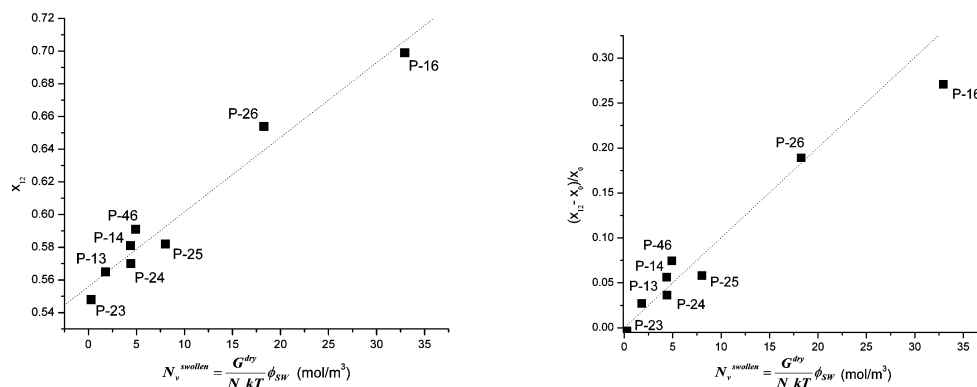


Figure 13. Left: Flory–Huggins parameters for samples P-13, P-14, P-16, P-23 to P-26, and P-46. They show a linear dependence on the cross-link molar density. Right: Plot of the reduced Flory–Huggins parameter vs the cross-link molar density. Please note that sample P-16 (that with the highest cross-link density) was excluded from fitting and therefore the results should be considered valid only at low or moderate cross-link densities.

Equation IV can be rearranged to provide the interaction parameter:

$$\chi_{1,2} = \frac{(V_1/\bar{v}M_C)(\phi_{sw}^{1/3} - \phi_{sw}/2) - \phi_{sw} - \ln(1 - \phi_{sw})}{\phi_{sw}^2}$$

By plotting it as a function of the volume fraction (Figure 12, left), a linear behavior is obtained. It should be noted that, even if this phenomenon is not described by the classic Flory–Rehner approach, this dependence of the Flory–Huggins parameter is frequently encountered for networks swollen both in organic solvents¹⁸ and water.¹⁹

Since the volume fraction linearly depends on the cross-link density, so should also the Flory–Huggins parameter, as previously reported in literature, specifically in the discussion by McKenna,¹⁸ which we will follow hereafter. We here prefer to quantify the dependence of $\chi_{1,2}$ on the cross-link density of the swollen networks, which, due to their substantially affine nature of the network, can be calculated from that of the corresponding dry state (easier to measure), by dividing this value by the volume swelling ratio, i.e., multiplying it by the polymer volume fraction:

$$N_v^{\text{swollen}} = \frac{G^{\text{dry}}}{N_a k T} \phi_{sw}$$

In particular, we would like to adopt here McKenna's approach for modeling the $\chi_{1,2}$ dependence on N_v^{swollen} : as a first step, we take the intercept of the $\chi_{1,2}$ vs $\chi_{1,2}^0$ plot with the Y axis ($\chi_{1,2}^0$) as the extrapolation of $\chi_{1,2}$ to zero cross-link density \cong infinite dilution (Figure 13, left).

The $\chi_{1,2}^0$ value is reportedly slightly higher (0.01–0.02¹⁸) than that of the uncross-linked, soluble polymer χ_u , which we can therefore estimate as $\chi_{1,2}^0 \approx 0.55 > \chi_u (=0.53\text{--}0.54)$. $\chi_{1,2}^0$ could then be used to derive a solvent-independent coefficient, α , that relates the Flory–Huggins parameter of a network to its cross-linking density in a “universal” (=non-dichloromethane-dependent) fashion: $(\chi_{1,2} - \chi_{1,2}^0)/\chi_{1,2}^0 = \alpha N_v = \alpha\{G/N_a k T\}$. The obtained value for α is $0.010 \pm 0.001 \text{ mol/m}^3$ (Figure 13, right).

Summary

We have prepared linear, bifunctional poly(propylene sulfide) macromonomers with a controlled amount of polymerizable end groups. These macromonomers were proved to effectively undergo photoactivated cross-linking, producing 3D networks

with elastomeric behavior; the rheological properties of the macromonomers during and after curing were easily predictable on the basis of the content of the polymerized groups and their distance.

In particular, the dry-state rheological behavior of these materials was shown to follow a simple affine chain scheme. In a solvent-swollen state, on the contrary, deviations from the classic Flory–Rehner theory were recorded, in that the Flory–Huggins interaction parameter was shown to be concentration-dependent. This result is not surprising and has been rationalized following an empirical concentration-dependent and therefore cross-link density-dependent model, which has been previously used for cross-linked natural rubber.¹⁸

Acknowledgment. The authors want to thank Micap plc (Runcorn, U.K.) for fundamental financial support, their enthusiasm, and freedom of research. BBSRC is gratefully acknowledged for financial support (Grant No. BBS/B/01537). N.T. is indebted to EPSRC for an Advanced Research Fellowship. The photopolymerization lamp, (L.E.Demetrion I) was kindly donated by KerrHawe, Switzerland.

References and Notes

- (1) Napoli, A.; Valentini, M.; Tirelli, N.; Müller, M.; Hubbell, J. A. *Nat. Mater.* **2004**, *3*, 183–189.
- (2) Rehor, A.; Hubbell, J. A.; Tirelli, N. *Langmuir* **2005**, *21*, 411–417.
- (3) Nicol, E.; Nicolai, T.; Durand, D. *Macromolecules* **1999**, *32*, 7530–7536.
- (4) Nguyen, K. T.; West, J. L. *Biomaterials* **2002**, *23*, 4307–4314.
- (5) Sawhney, A. S.; Pathak, C. P.; Hubbell, J. A. *Macromolecules* **1993**, *26*, 581–587.
- (6) Rehor, A.; Tirelli, N.; Hubbell, J. A. *Macromolecules* **2002**, *35*, 8688–8693.
- (7) Rehor, A.; Tirelli, N.; Hubbell, J. A. *J. Controlled Release* **2003**, *87* (1–3), 246–247.
- (8) Napoli, A.; Tirelli, N.; Kilcher, G.; Hubbell, J. A. *Macromolecules* **2001**, *34*, 8913–8917.
- (9) Bonnansplaisance, C.; Levesque, G.; Midrak, A. *Eur. Polym. J.* **1994**, *30* (2), 239–244.
- (10) Lutolf, M. P.; Tirelli, N.; Cerritelli, S.; Cavalli, L.; Hubbell, J. A. *Bioconjugate Chem.* **2001**, *12*, 1051–1056.
- (11) Shu, X. Z.; Liu, Y. C.; Palumbo, F. S.; Lu, Y.; Prestwich, G. D. *Biomaterials* **2004**, *25*, 1339–1348.
- (12) Becker, T. A.; Kipke, D. R.; Brandon, T. J. *Biomed. Mater. Res.* **2001**, *54* (1), 76–86.
- (13) Paavola, A.; Yliruusi, J.; Kajimoto, Y.; Kalso, E.; Wahlstrom, T.; Rosenberg, P. *Pharm. Res.* **1995**, *12*, 1997–2002.
- (14) Watts, D. C. *Dental Mater.* **2005**, *21*, 27–35.
- (15) Dossin, L. M.; Graessley, W. W. *Macromolecules* **1979**, *12*, 123–130.
- (16) Edwards, S. F.; Vilgis, T. A. *Rep. Prog. Phys.* **1988**, *51* (2), 243–297.
- (17) Flory, P. J.; Rehner, J. *J. Chem. Phys.* **1943**, *11*, 521.
- (18) McKenna, G. B.; Flynn, K. M.; Chen, Y. H. *Polymer* **1990**, *31*, 1937–1945.
- (19) Pfister, P. M.; Wendlandt, M.; Neuenschwander, P.; Suter, U. W. *Biomaterials* **2007**, *28*, 567–575.

MA070179Z